

Isolator Internal Resonance and Radiated Noise from Ships

Paul DYLEJKO¹; Ian MACGILLIVRAY²; Alex SKVORTSOV³

¹⁻³ Maritime Division, Defence Science and Technology Organisation, Australia

ABSTRACT

Reducing the radiated noise from ships is becoming increasingly important as ship-builders aim to reduce the disturbance to marine life, passengers and crew. A major contributor is on-board machinery which typically radiates noise to the water column from both structure-borne and air-borne transmission paths. Problematic machinery is often decoupled from the hull by supporting it on resilient isolation mounts. This paper predicts the effect of isolator internal resonance on the underwater radiated noise by considering a typical marine diesel characterised by source levels estimated from empirical relationships. The structure-borne and air-borne transmission paths are resolved individually using approximate analytical methods. It is subsequently demonstrated that the reduction of isolator internal resonances could provide a significant reduction in the underwater radiated noise from ships.

Keywords: Ship, Noise, Isolator

I-INCE Classification of Subjects Numbers: 13.5, 46.2

1. INTRODUCTION

Machinery noise and its transmission is an important factor in the design of just about any engineered structure. Buildings, ships, and cars are all subject to limitations on the allowable noise for a variety of reasons. For example, for fisheries research vessels, the International Council for the Exploration of the Seas (ICES) has recommended maximum levels of underwater radiated noise to minimise disturbance to marine life and improve acoustic survey capability (1). In this context, the ability to estimate the radiated noise from noisy machinery components is highly desirable, especially in the concept design stage. Noise reduction measures are cheaper and best implemented during the design phase rather than retro-fit (2).

For ships, a significant source of noise is the engines. The main transfer paths into the ship structure, demonstrated in Figure 1, can be broken down into the resilient mountings [1], surrounding air [2], pipes [3], propulsion system [4] and the resiliently mounted exhaust system [5] (3). From these transfer paths, the most significant noise mechanisms are normally the structure-borne noise from the resilient mounts [1] and the noise transmission through the surrounding air [2].

For radiated noise prediction, it is useful to consider the source, transmission path, and receiver independently. The definition of the source strength should allow for the consistent comparison of different sources; comparison of sources with set limits; prediction of noise levels when installed; and quantification of improved low noise designs (4). For the airborne path, sound power meets these criteria and is readily measured and has been standardized (5). For the structure-borne path, free-velocity has been used, with reasonable accuracy, for predicting the radiated noise from machinery (6). When it comes to the transfer paths for ship noise, these have usually been quantified with a combination of statistical energy analysis, computational methods and empirical relationships (2, 3, 7-11).

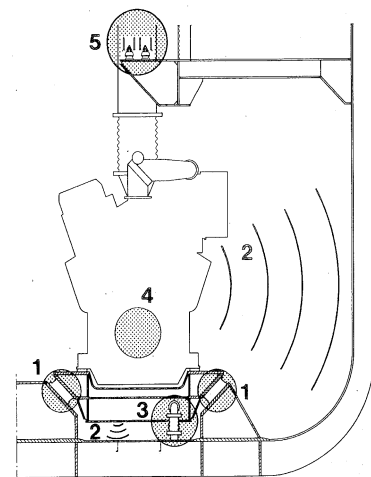


Figure 1 – Marine engine noise sources (3)

¹ paul.dylejko@dsto.defence.gov.au

² ian.macgillivray@dsto.defence.gov.au

³ alex.skvortsov@dsto.defence.gov.au

The accuracy of traditional methods of predicting ship noise can be within 3–5 dBA (7). However, the errors with narrow band predictions can be as much as 10 dB. The difficulties in predicting noise levels are related to the over-simplification of complex systems and the inherent variability associated with manufacturing processes and constituent materials. Plunt (7) noted that two nominally identical ships were found to differ by as much as 3 dBA. Representing levels in octave-bands reduces the variability but sacrifices resolution. Nonetheless, these approximate techniques still provide reasonable accuracy for broad evaluation of mitigation strategies.

Isolator internal resonances have been shown to increase power transmission and subsequently radiated noise from simple structures (12, 13). The focus of this paper is to investigate the relative importance of vibration isolator internal resonance on underwater noise radiated from ships. A case study with a typical marine diesel engine is characterized by its sound power and free-velocity derived from empirical relationships. The exhaust noise is not considered since this is usually radiated above water. Consequently, the large impedance mismatch at the air-water boundary results in a negligible proportion of the exhaust noise being transmitted into the water column.

The *structure-borne* noise is evaluated considering an equivalent rigid lumped mass and uni-axial isolation system. The blocked force is calculated under the assumption that the foundation impedance is much larger than that of the engine. This allows for the radiated noise in the water to be approximated by applying the resulting force to an infinite plate representation of the hull. This approximation has been proven to provide good correlation with the mean radiated noise level from an applied force against a wetted ship hull (14).

The *air-borne* noise is resolved by considering an energy-based framework. The transmitted sound power is broken down into the reverberant and direct fields. These fields are functions of the compartment volume, air absorption and wall reflection and transmission properties. The wall properties are determined using a transmission matrix approach.

Finally, the relative contributions of the air-borne and structure-borne paths are investigated and the contribution of the isolator internal resonances to the overall noise level is evaluated and discussed. Although these techniques do not consider much of the finer detail, they still demonstrate the broader trends which are also seen in more complicated models.

2. METHODOLOGY FOR PREDICTING RADIATED NOISE

A basis for predicting the radiated noise from a structure is to consider the problem in terms of a source-path-receiver framework, such as the description shown in Figure 2.

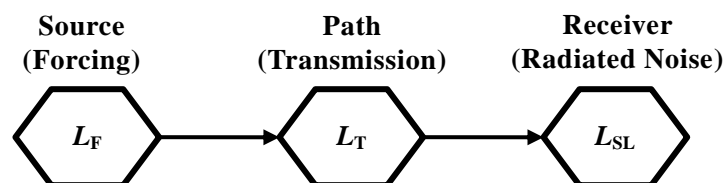


Figure 2 – Schematic of a source-path-receiver description

In this case the source, transmission path and receiver are represented by the levels L_F , L_T and L_{SL} respectively. These levels will often be represented by reduced data sets which may not include all possible detail or available resolution. For example, in the early stages of concept design it is assumed that the source levels are most likely available as octave or one-third-octave band frequency spectra. These spectra represent the power summed over a constant percentage bandwidth and as such will often “smear out” narrow-band features such as resonances. The transmission path level L_T should also be of an equivalent frequency resolution and fidelity. For levels in dB, referenced to appropriate units, the receiver level can be calculated within a particular frequency band by summing the source and transmission path levels.

The individual components of the transmission path can be evaluated entirely in narrow-band. The final transmission path level L_T , however, should be consistent with the source level L_F . A reasonable method for calculating the reduced transmission path level is to average the linear (not in dB) power or square of the representative transfer function over the appropriate frequency bandwidths. The resulting radiated noise level can be estimated from

$$L_{SL} = L_F + L_T \quad (\text{dB, re } = 1 \mu\text{Pa}^2/\text{Hz at 1 m}) \quad (1)$$

A reasonable high frequency approximation is to assume that each path is incoherent and can be

treated independently. The resulting noise level is determined by summing the intensities of the independent paths,

$$L_{\text{SL}}^{\text{Total}} = 10 \log_{10}(10^{L_{\text{SL}}^{\text{S}}/10} + 10^{L_{\text{SL}}^{\text{A}}/10}) \quad (\text{dB, re } = 1 \mu\text{Pa}^2/\text{Hz at 1 m}) \quad (2)$$

where L_{SL} is the predicted radiated noise spectrum level. The superscripts are used to associate the noise levels with either the *structure-borne* (S) or *air-borne* (A) paths. Spectrum level is defined as the power spectral density with a one Hz frequency spacing (15). This quantity is commonly used when describing the acoustic source level of ships.

3. STRUCTURE-BORNE NOISE

Empirical relationships have been previously developed for estimating the free-velocity of common marine diesels. The free-velocity of a rigid diesel engine of mass m_E in kg, power P in kW and rated speed s_0 in rpm can be estimated from (8, 9)

$$L_{\text{F}}^{\text{S}} = \Delta L_V - 20 \log_{10} m_E + 20 \log_{10} P + 30 \log_{10} s/s_0 + 122 \quad (\text{dB, re } = 5 \times 10^{-8} \text{ m.s}^{-1}) \quad (3)$$

where s is the speed of operation and ΔL_V is a frequency correction given in Table 1.

Table 1 – Frequency correction for Equation (4) (8, 9)

f_c (Hz)	16	31.5	63	125	250	500	1000	2000	4000	8000	16000
ΔL_V (dB)	0	-3	-4	-4	-5	-6	-6	-10	-18	-29	-44

An approximate transfer function for converting the free-velocity into an equivalent uni-axial force spectrum level can be written as

$$L_{\text{X}} = 20 \log_{10} 2\pi f_c m_E - 10 \log_{10} \Delta f_{\text{OB}} - 146 \quad (\text{dB, re } = 1 \text{ N}/5 \times 10^{-8} \text{ m.s}^{-1}/\text{Hz}) \quad (4)$$

where f_c and Δf_{OB} are the centre frequency and bandwidth in Hz for the octave band under consideration. This expression assumes that the engine behaves as a rigid mass.

Critical machinery such as a marine diesel can be hard mounted, or supported on either 1-stage or 2-stage isolation systems incorporating resilient elements. These elements, typically made of rubber or other viscoelastic materials, reduce transmitted vibration by dissipating and impeding the transfer of vibrational energy. A uni-axial transmission model is suitable in this case since the source level is also one-dimensional. Any additional complexity would potentially introduce artefacts or errors associated with the interpretation of the source from the coupling to other dimensions.

The transmissibility of the diesel-isolation system can be calculated using the transmission matrix method (16). A schematic of a transmission matrix model of a two-stage isolation system is shown in Figure 3. The transmission matrices α^m for a lumped mass, α^k for an ideal stiffness, and α^l for a resilient element represented as a slender rod, are given in Equations (5) to (7). These individual elements, which relate force f and velocity v , can be derived from analytical, computational or experimental methods. The system matrix β can be built up with any number of stages by the forward multiplication of the transmission matrices of the constituent elements, as shown in Equation (8). In these expressions, ω , m , A , E and l respectively represent angular frequency (in rad/s), mass, cross sectional area, Young's modulus and isolator length. The longitudinal wavenumber is given by $k_L = \omega/c_L$, where $c_L = \sqrt{E/\rho}$ and ρ is density. Hysteretic damping is included by using a complex Young's modulus $E(1 - j\eta)$, where η is the loss factor. As a first approximation, the foundation impedance is assumed to be much larger than the impedance at the engine mountings; the transmissibility T_F is simply the inverse of the first element of the system matrix, as shown in Equation (9). In line with this assumption, the resulting force can be applied directly to the hull.

A good approximation to the mean radiated noise from a ship hull excited by a point force below the critical frequency (typically above 4 kHz) is obtained by considering an infinite, homogenous flat plate of the same thickness and material as the hull plate (14, 17). The expression T_P relating the normal sound pressure, referenced to 1 m, to a unit force applied to the hull, is given in Equation (10). Quantities ρ_s , ρ_f and h are respectively the density of the hull, density of the fluid and hull thickness. The fluid wavenumber is $k_f = \omega/c_f$, where c_f represents the speed of sound in water. This expression is simple because it describes the radiated pressure associated with the near-field deflection. The component of radiated noise from the propagating components, below the critical frequency, is

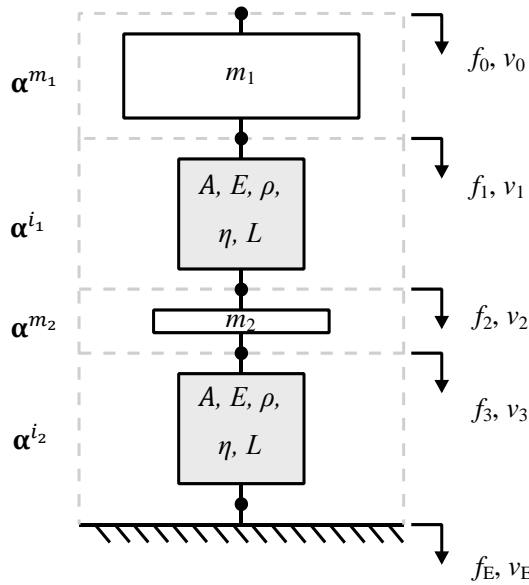


Figure 3 – Schematic of the model for the structure-borne path

$$\alpha^m = \begin{bmatrix} 1 & -j\omega m \\ 0 & 1 \end{bmatrix} \quad (5)$$

$$\alpha^k = \begin{bmatrix} 1 & 0 \\ -j\omega l & 1 \end{bmatrix} \quad (6)$$

$$\alpha^i = \begin{bmatrix} \cos(k_L l) & \frac{-AEk_L \sin(k_L l)}{-j\omega} \\ \frac{-j\omega \sin(k_L l)}{AEk_L} & \cos(k_L l) \end{bmatrix} \quad (7)$$

$$\beta = \alpha^{m_1} \alpha^{i_1} \quad \text{or} \quad \beta = \alpha^{m_1} \alpha^{i_1} \alpha^{m_2} \alpha^{i_2} \quad (8)$$

$$T_F = \frac{f_E}{f_0} = \beta_{11}^{-1} \quad (9)$$

$$T_P = \frac{-j k_f e^{jk_f h}}{2\pi(1 - jk_f h \rho_s / \rho_f)} \quad (10)$$

negligible due to the short wavelengths when compared with the fluid wavelength (14).

Finally, the mathematical definition of the structure-borne transfer function is given as

$$L_T^S = L_X + 10 \log_{10} \langle |T_F T_P|^2 \rangle_{OB} + 120 \quad (\text{dB, re } = 1 \mu\text{Pa}^2/\text{N at 1 m}) \quad (11)$$

$\langle \rangle$ is used to designate an average quantity; the subscript, in this case, signifies that the average is taken over the relevant octave band.

AIR-BORNE NOISE

As with the structure-borne noise, empirical relationships have been developed for estimating the radiated sound power from typical marine diesels (8, 9). The source level for the air-borne path L_F^A can be written as

$$L_F^A = \Delta L_A + 58 + 10 \log_{10}(P) \quad (\text{dB, re } = 1 \text{ pW}) \quad (12)$$

where ΔL_A is the frequency correction including intake noise.

Table 2 – Frequency correction for Equation (12) (8, 9)

f_c (Hz)	31.5	63	125	250	500	1000	2000	4000	8000
ΔL_A	13	21	28	28	27	29	28	22	15

In order to estimate the radiated noise from a hull compartment of volume (V) due to the air-borne path an energy-based theoretical framework, consistent with room acoustics, is developed. A pictorial representation of the individual components of the air-borne path is presented in Figure 4. To calculate the noise radiation based on energy considerations both the reflection and transmission properties of the boundary wall are needed. The transfer function of total power radiated to the exterior of the compartment can be separated into the reverberant and direct components according to

$$\Pi_{OUT} / \Pi_S = \dot{\Pi}_R + \dot{\Pi}_D \quad (13)$$

where Π_{OUT} / Π_S is the ratio of the underwater acoustic power and the source acoustic power. $\dot{\Pi}_R$ and $\dot{\Pi}_D$ are the components of this ratio associated with the reverberant and direct fields respectively. The dash is used to indicate that these quantities are normalized by the source acoustic power. The reflection controls the build-up of the reverberant field in the compartment and the transmission controls how much of the direct and reverberant fields pass to the exterior.

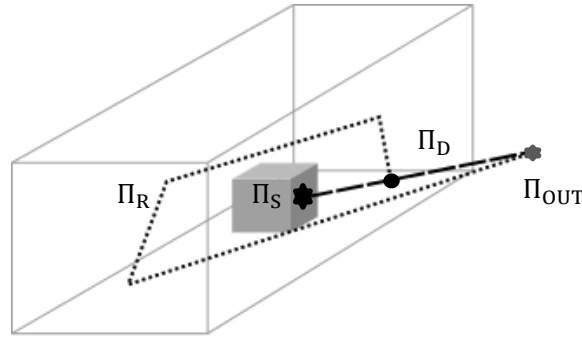


Figure 4 – Constituents of the airborne path

The normalized reverberant and direct components of the output power can be written as

$$\dot{\Pi}_R = \langle \beta \rangle S c_a \langle \epsilon'_R \rangle / 4 \quad (14) \quad \dot{\Pi}_D = \langle \beta \rangle S c_a \langle \epsilon'_D \rangle / 2 \quad (15)$$

Where $\langle \beta \rangle$, S , c_a and $\langle \epsilon \rangle$ are, respectively, the average wall energy transmission coefficient, wall surface area, sound speed of the compartment air, and the average energy density per unit input power. As only half the flux from the reverberation acts towards the wall and the average normal component of that is also halved when averaged over all incident directions, the net flux of the reverberant field onto the compartment wall is $c_a \langle \epsilon'_R \rangle / 4$. For the direct field component of the energy density, the direct flux onto the wall will depend on the source position. Averaging over all source positions, the normalized outward flux of the direct-field energy density can be approximated by $c_a \langle \epsilon'_D \rangle / 2$. At equilibrium, the power produced is balanced by the volume and wall surface losses (the latter including wall absorption as well as outward transmission).

Balancing power, the energy densities of the reverberant and direct fields can be written as

$$\langle \epsilon'_R \rangle = \frac{1 - \langle \alpha \rangle}{\gamma V + \langle \alpha \rangle c_a S / 4} \quad (16) \quad \langle \epsilon'_D \rangle = \frac{1}{\gamma V + c_a S / 2} \quad (17)$$

In these expressions γ and $\langle \alpha \rangle$ represent the frequency dependent volume attenuation and the average energy absorption coefficient of the wall surface as per Beranek (18). The volume attenuation γ is related to the volume absorption coefficient η , in Np/m, and η_D , in dB/m, of the interior fluid (see Landau and Lifshitz (19)) according to

$$\gamma = \eta / 2c_a \quad (18) \quad \eta = \eta_D \ln(10) / 20 \quad (19)$$

The wall absorption coefficient $\langle \alpha \rangle$ and the average transmission coefficient $\langle \beta \rangle$ to the exterior space for a wall composed of different surfaces, specified by index i , are given by

$$\langle \alpha \rangle = \sum_i S_i (1 - R_i) / S \quad (20) \quad \langle \beta \rangle = \sum_i (S_i T_i) / S \quad (21)$$

where $S = \sum_i S_i$ and R_i and T_i represent the incidence-angle-averaged, frequency-dependent, reflection and transmission coefficients R and T of wall i . These coefficients also depend on wall properties such as thicknesses, densities and elastic constants (including absorption terms) of the materials composing the wall. For non-wetted portions of the hull where the sound can be assumed not to enter the water T_i would be set to zero, but this level of detail has not been used in the case study.

In the case of the reverberant field the conventional field-incidence angle average of R , $\langle R \rangle_{FI}$, is appropriate for R_i with $\langle T \rangle_{FI}$ also used for T_i . For the direct field the required average of T is not well defined. For example, if the source is located in the centre of a sphere, the average of T is the normal incidence value. However, Equation (17) is an average and the source position is unknown, so it will be assumed that the direct field average of T can be approximated by $\langle T \rangle_{FI}$ and used as T_i also, so that $\langle \beta \rangle$ factors in Equations (14) and (15) have the same frequency-dependent value.

Propagation of waves in layered absorbing elastic materials has been well studied (20-23). Typical solution methods involve an approach for the reflection and transmission of plane waves where each layer is represented by a transmission matrix. Unlike a uniaxial system involving force and velocity, where each element is a 2×2 transmission matrix (the so-called 4-pole parameters), the transmission matrices for elastic materials involve shear stress and shear displacement. In the Brekhovskikh (21) theory, for example, each matrix is a 4×4 matrix involving angle of incidence of the sound, the layer thickness, density, complex compressional velocity and complex shear velocity, where the complex

parameters account for absorption. The angle and frequency-dependent reflection and transmission coefficients, R and T , are obtained from the appropriate elements of the final product of the matrices, as with standard 4-pole techniques, although the equations describing the problem can be quite complex.

Finally, the air-borne transfer function level can be calculated by

$$L_T^A = 10 \log_{10}(\dot{P}_R + \dot{P}_D) + 10 \log_{10} c_f \rho_f / 4\pi - 10 \log_{10} \Delta f_{OB} \quad (\text{dB, re } = 1 \mu\text{Pa}^2/\text{pW/Hz at 1 m}) \quad (22)$$

The second term of this equation converts to sound pressure, assuming a monopole source radiating into a full space, the third term converts to spectrum level. For radiation into a half-space the level would be 3 dB higher.

4. CASE STUDY

A case study is developed to study the potential importance of isolator internal resonances on the underwater noise radiated from a ship. A typical 10 tonne 1 MW marine diesel is considered, supported on either a 1-stage or 2-stage mounting configuration in a compartment with a volume of 150 m³ and surface area of 190 m². The intermediate mass for the 2-stage system is conservatively chosen to be 10% of the primary mass. A typical noise attenuating internal cladding is considered, made up of an outer perforated steel plate, fibreglass layer and 25 mm air gap. The hull thickness h , hull density ρ_S , water density ρ_f and water sound-speed c_f are assumed to be 5 mm, 7800 kg/m³, 1000 kg/m³ and 1500 m/s respectively. The remaining parameters for the case study are given in Table 3.

Table 3 – Case study parameters

Isolators		Air		Fibreglass		Perforated Plate	
A	0.04 m ²	Sound-speed	343 m/s	Thickness	25 mm	Thickness	1 mm
E	5 MPa	Density	1.25 kg/m ³	Density	48 kg/m ³	Porosity	0.05
ρ	1250 kg/m ³	Viscosity	20×10 ⁻⁶ Pa.s	Diameter	9 μm	Diameter	1 mm
l	0.107 m	Temperature	25 °C				
η	0.10	Humidity	50%				

The structure-borne and air-borne octave-band source levels L_F^S and L_F^A calculated from Equations (3) and (12) are plotted in Figure 5. The narrow-band force transmissibility T_F for the diesel supported on either a 1-stage or 2-stage isolation system and the radiated noise from a unit point force on the hull T_P are presented in Figure 6. The transmissibility responses are also shown for ideal springs (no internal resonances, IRs). The rigid body resonance for the 1-stage system is around 6 Hz. The 2-stage rigid body resonances are approximately 4 Hz and 28 Hz. The first internal resonance occurs around 300 Hz. The transmissibility falls-off at a rate of 12 and 24 dB per octave for the ideal 1-stage and 2-stage systems respectively. The introduction of the internal resonances halves this rate when considering the response between resonances. The radiation efficiency of the hull increases at a rate of roughly 6 dB per octave over much of the frequency range.

For the air-borne path, the reflection and transmission coefficients R and T have been modelled numerically by implementing the theory of Lévesque and Piché (23). Field incidence values of R and T have been computed for incidence angles up to 78°. This theory is only valid for frequencies where sound incident on the layered surface can be treated using plane-wave theory, which implies that the dimension or radius of curvature of the compartment wall should significantly exceed the wavelength of sound. For an interior air space of spherical volume with radius 3 m, for example, those frequencies would be greater than 100 Hz. The volume absorption coefficient of air is computed for the given temperature and humidity using the formula of Bass *et al.* (24), agreeing closely with the tabulated data of Bies and Hansen (25). Porous fibrous materials are modelled by computing the flow resistivity based on a specific bulk density of the material and the fibre diameter (see, for example, Bies and Hansen (25)). The theory of Delany and Bazley (26) is used to convert the flow resistivity into the material impedance. This impedance, coupled with the complex density, is incorporated into the multi-layer reflection and transmission modelling.

The perforated plate has been modelled using the transfer impedance theory of Maa (27) using the correction of Fok as used in the reference (28). The transfer impedance is converted into absolute

impedance by determining equivalent fluid properties for a plate of given thickness, porosity and hole perforation diameter, for inclusion in the multi-layer reflection and transmission modelling. The plate is otherwise assumed rigid.

The spectrum level, in octave-bands from 63 Hz to 4 kHz, from individual paths for several different scenarios, is shown in Figure 7. The structure-borne scenarios, in descending order of dominance, have isolation systems with 1-stage, 1 ideal stage, 2-stages and 2 ideal stages. The air-borne scenarios, in descending order of dominance, include air absorption, 50% coverage of the internal surface area with cladding, and 100% coverage.

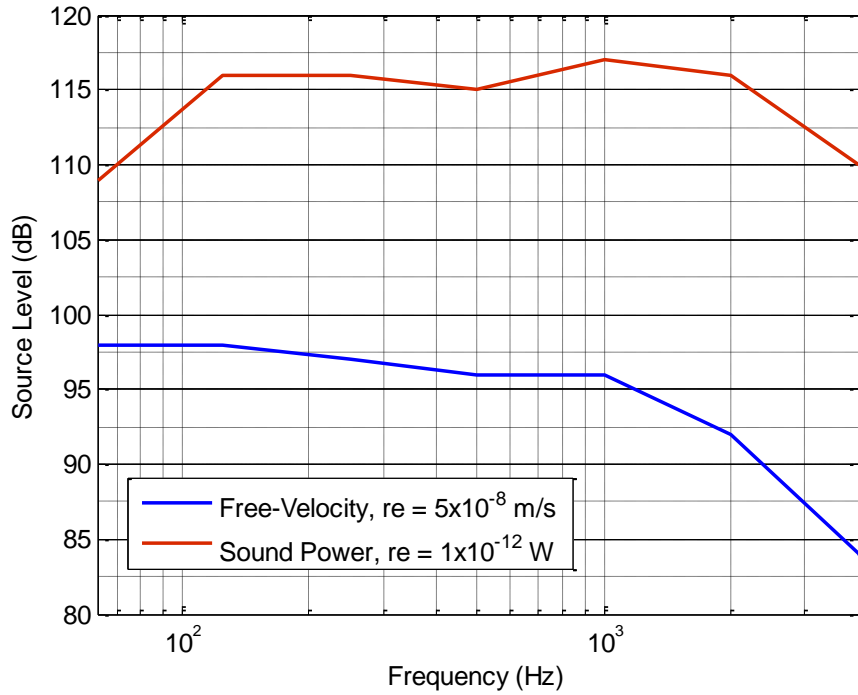


Figure 5 – Candidate engine source characteristics

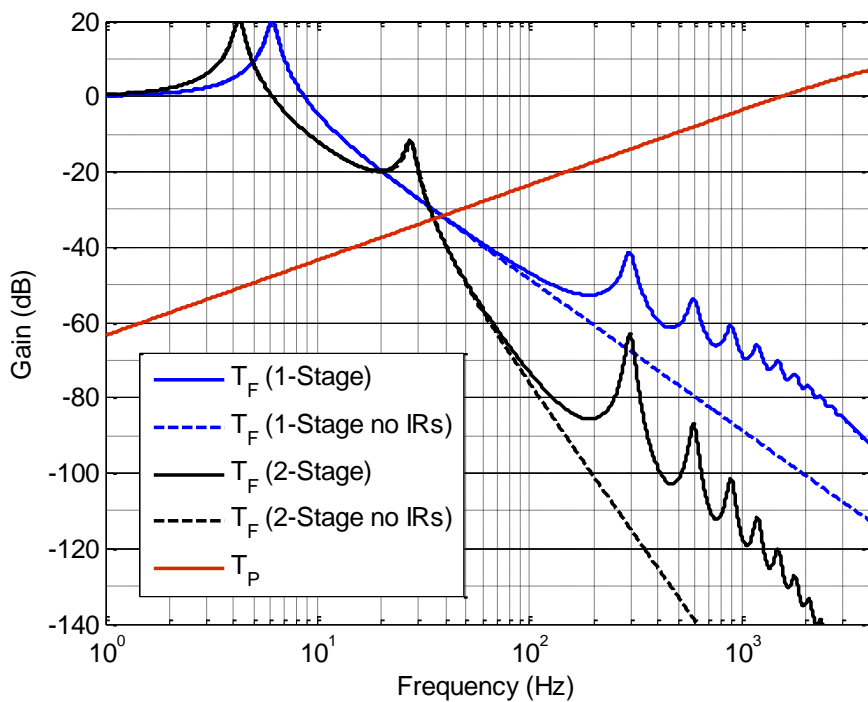


Figure 6 – Transfer function gains for the isolation systems and hull radiated noise

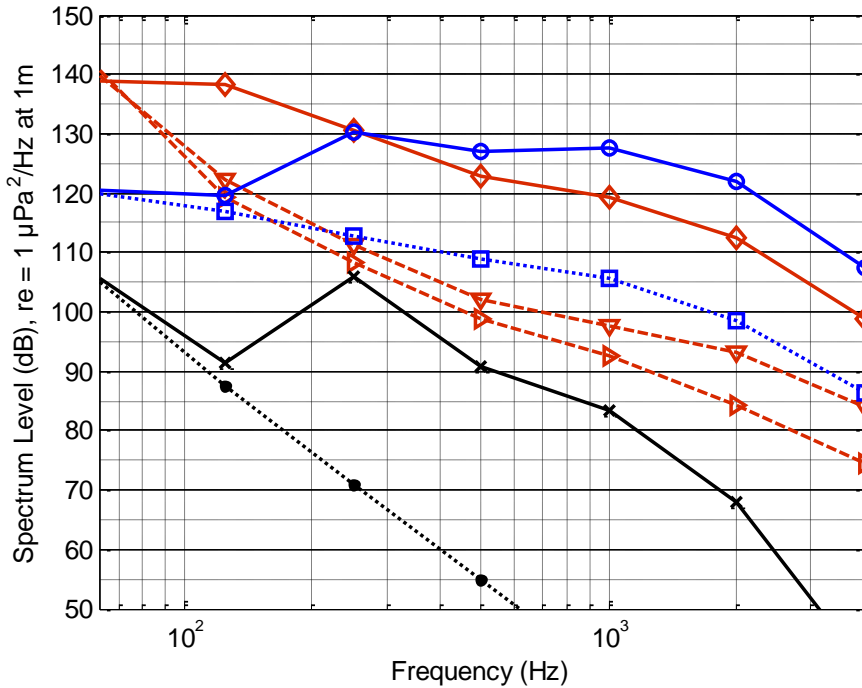


Figure 7 – Radiated noise from individual cases in descending high-frequency dominance: structure-borne 1-stage $\text{---}\circ\text{---}$, air-borne with air absorption $\text{---}\diamond\text{---}$, structure-borne 1-stage no IRs $\text{---}\square\text{---}$, air-borne with absorptive coating 50% coverage $\text{---}\nabla\text{---}$, air-borne with absorptive coating 100% coverage $\text{---}\blacktriangledown\text{---}$, structure-borne 2-stage $\text{---}\times\text{---}$ and structure-borne 2-stage no IRs $\text{---}\blacklozenge\text{---}$.

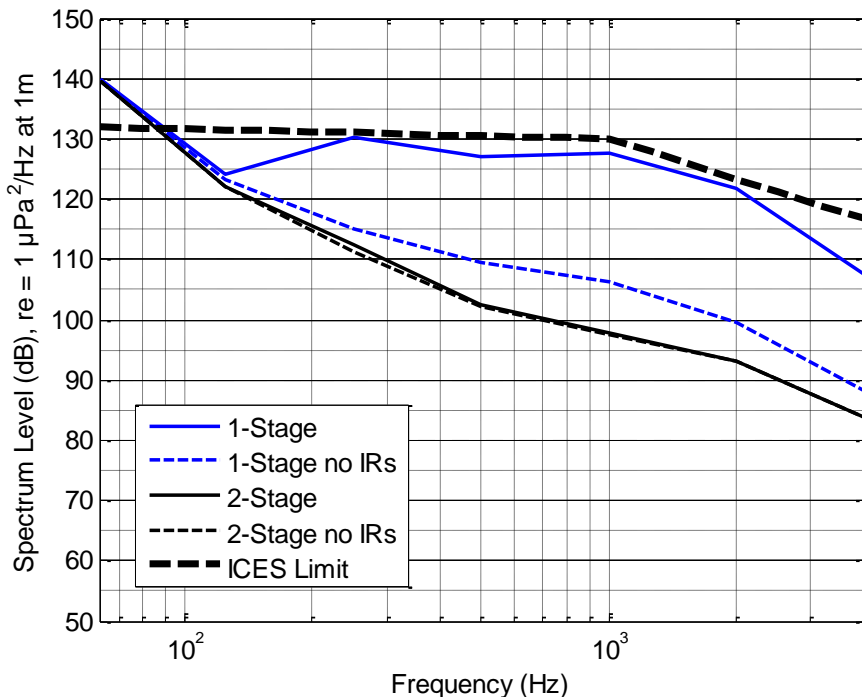


Figure 8 – Total radiated noise considering different isolation systems with and without IRs

Examining the structure-borne path, the internal resonances for the 1-stage and 2-stage isolation systems increase the radiated noise by as much as 23 dB and 46 dB respectively. It should be acknowledged, however, that this 2-stage system represents a worst case since the same isolators were used in both stages. Using different isolators with different internal resonance frequencies would smear their effect over a wider frequency range.

Although not shown explicitly, for the air-borne path, it is worth noting that the loss due to air absorption is significant, especially at higher frequencies. This is associated with the high reflectivity of the steel hull which results in sound travelling a great distance, on average, before exiting the hull. The addition of 50% noise attenuating cladding drops the radiated noise by as much as 20 dB. By coating the whole surface, the radiated noise is further reduced, especially at high frequencies, by as much as 9 dB.

The total radiated noise is plotted in Figure 8, including sound-attenuating cladding covering 50% of the surface area, and considering both a 1-stage and 2-stage isolation system with and without internal resonances. For context, the underwater noise limit suggested by ICES (1) is also included. For the 1-stage system modelled here, the internal resonances increase the radiated noise by as much as 22 dB for frequencies above 250 Hz. The 2-stage system is better at reducing the radiated noise. Significantly, there is little impact from the internal resonances. The 2-stage system provides up to 10 dB greater noise reduction when compared with the idealized 1-stage system and the dominant path is now air-borne.

5. CONCLUSIONS

This paper has put forward a methodology for predicting the underwater machinery noise from ships. The air-borne and structure-borne paths were considered separately by assuming their contribution to the total radiated noise was incoherent. A case study was developed to examine the contribution of isolator internal resonances to the underwater noise from a typical marine diesel which was characterized by empirical relationships. The structure-borne noise was determined by considering a rigid foundation and a uni-axial transmission matrix model with an infinite-plate representation of the hull. A rigid termination has been previously shown to be a reasonable approximation for determining the transmitted force when the foundation impedance is much larger than the engine impedance. The estimation of the underwater radiated noise, below the critical frequency, by considering a point excited infinite plate was also in line with previous studies. The air-borne noise was modelled using an energy-based framework which divided the sound power into the reverberant and direct fields. The transmission through the hull was determined using a transmission matrix approach.

The results from the case study demonstrated that with noise attenuating cladding and a 1-stage isolation system, the structure-borne path dominated much of the frequency range. Failure to consider the internal resonances under-predicted the total radiated noise level by as much as 22 dB. With the 2-stage isolation system, the air-borne path was dominant. These results show that, for a 1-stage isolation system, isolator internal resonance could be a significant contributor to the underwater noise and should be considered. The study has also shown that elimination of the internal resonances in a 1-stage system could result in underwater noise levels approaching those of a two stage system without the added mass and complexity.

ACKNOWLEDGEMENTS

The authors would like to thank Christopher Norwood for many useful comments and suggestions.

REFERENCES

1. Miston RB. Underwater noise of research vessels review and recommendations. ICES Cooperative Research Report 209, 1995.
2. Andresen K, Nilsson AC, Brubakk E. Noise prediction and prevention. Proceedings of the 2nd International Symposium on Shipboard Acoustics ISSA '86; October 7-9; The Hague, The Netherlands: 1986.
3. Verheij JW. Multi-path sound transfer from resiliently mounted shipboard machinery. The Netherlands: Institute of Applied Physics TNO-TH; 1986.
4. Moorehouse AT. On the characteristic power of structure-borne sound source. *Journal of Sound and Vibration*. 2001;248(3):441-59.
5. International Standard: ISO 9611 - Acoustics – Characterization of structure-borne sound with respect to sound radiation from connected structures – Measurement of velocity at the contact points of machinery when resiliently mounted: 1996.
6. Gibbs BM. Uncertainties in predicting structure-borne sound power input into buildings. *Journal of the Acoustical Society of America*. 2013;133(5):2678-89.

7. Plunt J. Methods for Predicting Noise Levels in Ships: Experiences for Empirical and Sea Calculation Methods. Part I. Noise Level Prediction Methods for Ships, Based on Empirical Data: Chalmers University of Technology; 1980.
8. Crocker MJ. Handbook of acoustics. New York: John Wiley & Sons; 1998.
9. Fischer RW, Burroughs CB, Nelson DL. Design guide for shipboard airborne noise control. New York: The Society of Naval Architects and Marine Engineers; 1983.
10. Nisson AC, editor Noise prediction and prevention in ships. Ship Vibration Symposium; 1978 October 16-17; Arlington, Va.
11. Smith M. Prediction methodologies for vibration and structure borne noise. Alberta Acoustics and Noise Association Spring Conference; May; Banff: 2011.
12. Du Y, Burdisso RA, Nikolaidis E, Tiwari D. Effects of isolators internal resonances on force transmissibility and radiated noise. *Journal of Sound and Vibration*. 2003;268:751-78.
13. Sun L, Leung AYT, Lee YY, Song K. Vibrational power-flow analysis of a MIMO system using the transmission matrix approach. *Mechanical Systems and Signal Processing*. 2007;21:365-88.
14. Wolde TT. Reciprocity Experiments on the Transmission of Sound in Ships: Drukkerij Hoogland en Waltman; 1973.
15. Urick RJ. Principles of underwater sound. Los Altos Hills, California: Peninsula Publishing; 1983.
16. Dylejko PG, MacGillivray IR. On the concept of a transmission absorber to suppress internal resonance. *Journal of Sound and Vibration*. 2014;333(10):2719-34.
17. Donaldson JM. Reduction of noise radiated from ship structures. *Applied Acoustics*. 1968;1(4):275-91.
18. Beranek LL. Noise and vibration control. Washington: Institute of Noise Control Engineering; 1988.
19. Landau LD, Lifshitz EM. Fluid mechanics. Volume 6.: Butterworth-Heinemann; 1987.
20. Ainslee MA. Plane-wave reflection and transmission coefficients for a three-layered elastic medium. *Journal of the Acoustical Society of America*. 1995;97(1):680-3.
21. Brekhovskikh LM. Waves in layered media. New York: Academic Press; 1960.
22. Cervenka P, Challande P. A new efficient algorithm to compute the exact reflection and transmission factors for plane waves in layered absorbing media (liquids and solids). *Journal of the Acoustical Society of America*. 1991;89(4):1579-89.
23. Lévesque D, Piché L. A robust transfer matrix formulation for the ultrasonic response of multilayered absorbing material. *Journal of the Acoustical Society of America*. 1992;92(1):452-67.
24. Bass HE, Sutherland LC, Zuckerwar AJ, Blackstock DT, Hester DM. Atmospheric absorption of sound: Further developments. *Journal of the Acoustical Society of America*. 1995;97(1):680-3.
25. Bies DA, Hansen CH. Engineering noise control. London 1988.
26. Delany ME, Bazley EN. Acoustical characteristics of fibrous absorbent materials. Technical report, Report of the National Physical Laboratory - Aerodynamics division. 1969.
27. Maa D-Y. Potential of microperforated panel absorber. *Journal of the Acoustical Society of America*. 1998;104(1):2861-6.
28. Randeberg RT. Perforated panel absorbers with viscous energy dissipation enhanced by orifice design. Trondheim: Norwegian University of Science and Technology; 2000.